IEEE Photonics Journal
An IEEE Photonics Society Publication

Over 20-W Mid-Infrared Picosecond Optical Parametric Oscillator

Volume 7, Number 5, October 2015

Zhipeng Qin
Guoqiang Xie
Weiyang Ge
Peng Yuan
Liejia Qian

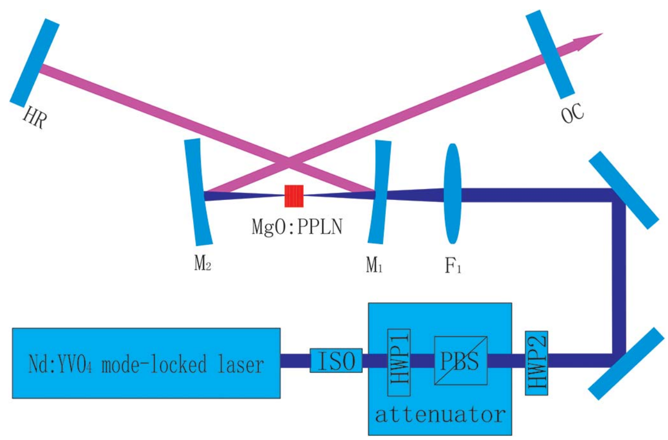

DOI: 10.1109/JPHOT.2015.2477281
1943-0655

Over 20-W Mid-Infrared Picosecond Optical Parametric Oscillator

Zhipeng Qin, Guoqiang Xie, Weiyang Ge, Peng Yuan, and Liejia Qian

Key Laboratory for Laser Plasmas (Ministry of Education) and Department of Physics and Astronomy, IFSA Collaborative Innovation Center, Shanghai Jiao Tong University, Shanghai 200240, China

DOI: 10.1109/JPHOT.2015.2477281

Manuscript received June 23, 2015; revised September 1, 2015; accepted September 2, 2015. Date of current version September 16, 2015. Corresponding author: G. Xie (e-mail: xiegq@sjtu.edu.cn).

Abstract: We report on a high-average-power mid-infrared picosecond optical parametric oscillator (OPO) synchronously pumped by a Nd:YVO_4 mode-locked laser. By use of the MgO-doped periodically poled $LiNbO_3$ as the nonlinear crystal, up to 20.2-W picosecond laser at 2128 nm was generated from the degenerate OPO, with a conversion efficiency of 66%. To the best of our knowledge, this is the highest mid-infrared average output power from synchronously pumped OPO so far. The output picosecond laser had a pulse duration of 29 ps and a pulse energy of 196 nJ, with an M^2 beam quality factor of 1.5. In the nondegenerate state operation, the signal power of 12.8 W at 1966 nm and the idler power of 10.5 W at 2319 nm were obtained, with a conversion efficiency as high as 76%. The high-average-power mid-infrared picosecond OPO may lead to the application of medical surgery, microprocessing of materials, etc.

Index Terms: Picosecond laser, mid-infrared (mid-IR) lasers, optical parametric oscillator.

1. Introduction

Rapid progress on the mid-infrared ultrafast laser (2–20 μm) has been driven by the potential demand for medical applications, gas sensing, breath analysis, trace gas detection, and spectroscopy because of the rotational–vibrational transition of many molecules in this spectral region [1]–[3]. In addition, the mid-infrared ultrafast laser is relevant for applications in mid-infrared supercontinuum generation, frequency down conversion, and material micro-processing of semiconductor, plastics, and composite materials [4]–[6].

At present, mid-infrared ultrashort pulses have been generated based on Tm (2.0 μm), Ho (2.1 μm), Cr (2.5 μm), or Er (2.9 μm) doped solid-state and fiber mode-locked lasers [7]–[10]. However, they suffer from problems of low average output power, narrow wavelength tuning range, and unavailable long wavelength output (> 3 μm). The synchronously pumped optical parametric oscillator (OPO) is a promising technique for generation of high-average-power, widely tunable mid-infrared ultrashort pulses. However, so far, mid-infrared average output power from synchronously pumped OPOs has been limited to the level of several watts [11]–[16].

In this paper, we have experimentally demonstrated a high-average-power mid-infrared picosecond-pulse OPO. With MgO:PPLN as nonlinear crystal and high-power Nd:YVO_4 mode-locked laser as pump source, the degenerate OPO emitted a maximum average output power of 20.2 W at 2.1 μm wavelength, with a conversion efficiency as high as 66%. The generated mid-infrared pulses had a pulse duration of 29 ps and repetition rate of 103 MHz, with a beam quality factor of 1.5. When operating in non-degenerate state, the synchronously pumped OPO

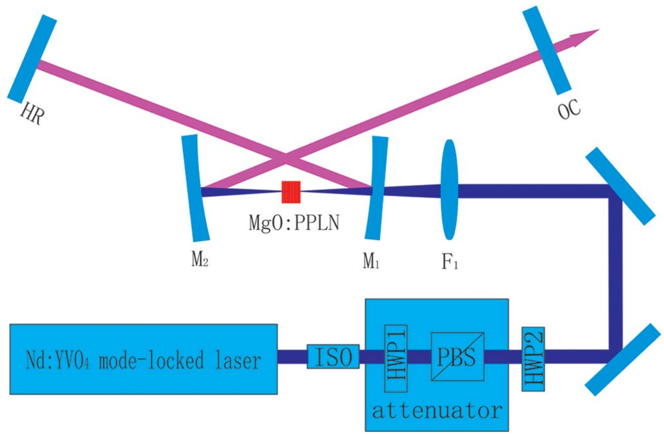

Fig. 1. Schematic of OPO synchronously pumped by a Nd:YVO_4 mode-locked laser. ISO: optical isolator; HWP: half-wave plate; PBS: polarizing beam splitter; HWP1 and PBS constitute the power attenuator.

emitted an average output power of 12.8 W at 1966 nm (signal) and 10.5 W at 2319 nm (idler) under a pump power of 30.8 W, corresponding to a conversion efficiency of 76%.

2. Experimental Setup

The schematic of synchronously-pumped OPO is shown in Fig. 1. A home-built large-mode-area Nd:YVO_4 mode-locked laser was adopted as the pumping source of OPO, which delivered a maximum average power of 39 W with pulse duration of 37 ps and repetition rate of 103 MHz at 1064 nm. Since a large laser mode (~1 mm) was adopted in the mode-locked Nd:YVO_4 laser, the output beam kept TEM_{00} mode even at the maximum output power. In order to eliminate the detrimental feedback, an Faraday isolator (Conoptics, Model 714) was positioned at the exit of the Nd:YVO_4 mode-locked laser and its damage threshold is 150 MW/cm^2, which is much larger than the incident peak intensity of 0.3 MW/cm^2. The half-wave plate (HWP1) and polarizing beam splitter (PBS) co-worked as power attenuator and the second half-wave plate (HWP2) was used to alter the light polarization from horizontal to vertical direction. In the experiment, a 50-mm length MgO:PPLN crystal was chosen as nonlinear OPO crystal because there is no limitation of the interaction length by spatial walk-off of the interacting waves when quasi-phase matching. The MgO:PPLN crystal (HCP, Taiwan) had a thickness of 1 mm and width of 8.6 mm with seven parallel-arranged gratings with periods ranging from 28.5 μm to 31.5 μm. The MgO: PPLN crystal temperature was controlled by an oven with an adjustable temperature range from room temperature to 200 °C. The MgO:PPLN crystal was anti-reflectively coated for pump, signal, and idler wavelengths, with reflectivity of $<0.5\%$ at 1064 nm, $<1\%$ from 1800 nm to 2500 nm. The plane-concave mirror M1, M2 and plane mirror M3 were high-reflectively coated with reflectance of $>99.5\%;$ from 1900 nm to 2200 nm. The output coupler was mounted on a translation stage with a transmission of 63%.

3. Results and Discussion

When the grating period of 31.5 μm was used and the MgO:PPLN temperature was set to be 200 °C, the OPO operated in degeneracy. In the experiment, through the doublet lens F1 ($f = 120$ mm) the pump light was imaged into the MgO:PPLN crystal with a waist radius of 40 μm. Based on the ABCD propagation matrix, the calculated cavity mode radius in MgO:PPLN crystal was 80 μm. Considering the wavelength effect on divergence, the pump and signal beam had the same divergence angle. In our case, the volume of cavity mode completely enclosed the pump beam in MgO:PPLN crystal and they had similar spot sizes at the ends of 50-mm-length

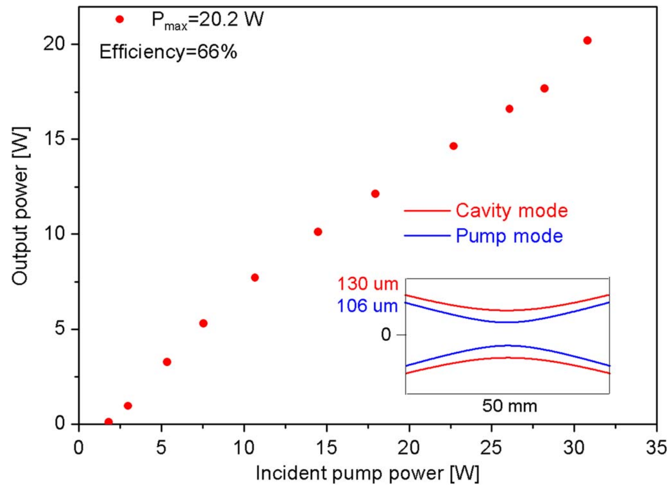

Fig. 2. Average output power versus incident pump power for the degenerate synchronously pumped OPO. (inset) Cavity mode and pump mode in the MgO:PPLN.

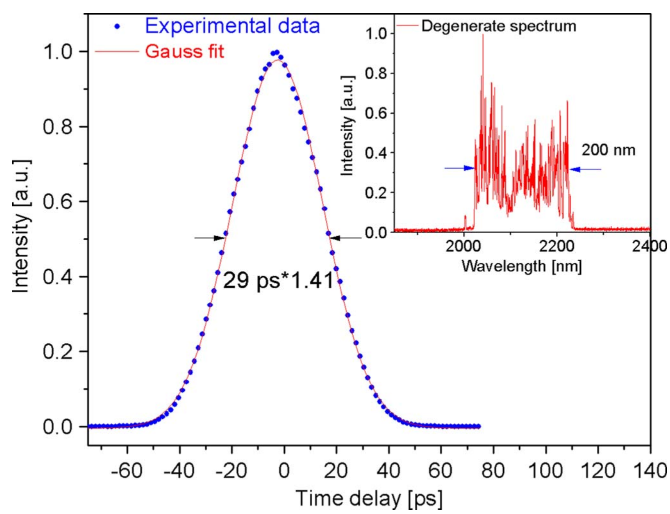

Fig. 3. Autocorrelation trace and spectrum of the output signal pulses from the degenerate OPO.

MgO:PPLN crystal for pump and signal beam (see the inset of Fig. 2). The cavity mode was slightly larger than the pump beam in the nonlinear crystal, which has two advantages: on one hand, it can sustain TEM_{00} mode operation of signal. On the other hand, the power density of signal is lower in the nonlinear crystal, which benefits to prevent back-conversion of OPO process in the saturation regime and achieve high OPO conversion efficiency. The output power characteristic of the synchronously-pumped OPO at degenerate operation is shown in Fig. 2. The threshold pump power for OPO oscillation was 1.8 W, corresponding to a peak optical intensity of 9.4 MW/cm^2. A maximum average output power of 20.2 W was obtained under a pump power of 30.8 W, corresponding to the conversion efficiency as high as 66%. At the pump power of 30.8 W, no damage occurred in the MgO:PPLN crystal. The higher average output power was only limited by the available pump power.

The intensity autocorrelation trace and spectrum of the signal pulses from the degenerate OPO are shown in Fig. 3. The pulse duration was measured by a commercial autocorrelator (APE, pulseCheck USB MIR). Assuming a Gauss-profile pulse, the pulse duration was 29 ps.

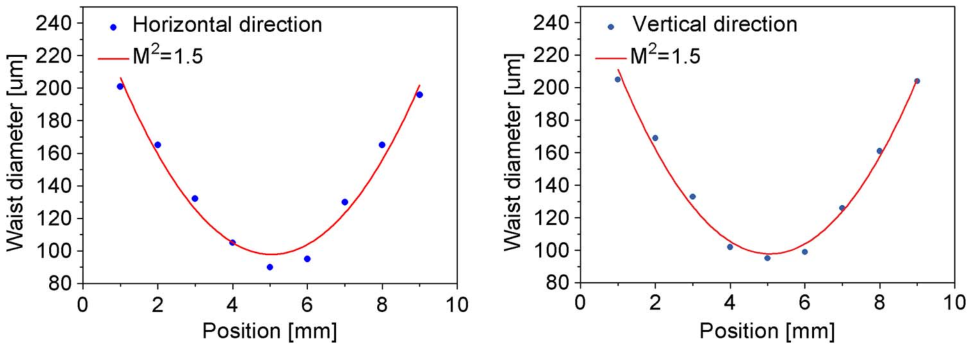

Fig. 4. Beam quality of signal pulses from the degenerate OPO at the maximum output power.

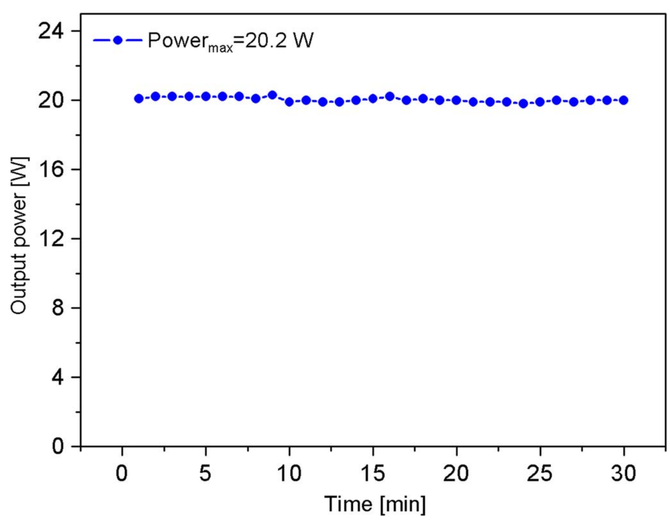

Fig. 5. Stability of the average output power for the degenerate OPO in half an hour.

The corresponding signal pulse spectrum, recorded by a mid-infrared spectral analyzer (Ocean Optics, SIR5000), is centered at 2128 nm with 200-nm bandwidth. The broad spectral bandwidth can be attributed to the extra wide phase-matching bandwidth in the degeneracy. The output pulses have a large time-bandwidth product value (~384), which implies low time coherence of the pulses.

The beam quality of signal pulses from the degenerate OPO at maximum output power was measured with the knife-edge method. We attenuated the high output power to 1 W with a 5%-coupler. Then the beam was focused by a doublet lens with a focal length of 75 mm. Along the beam propagation direction, we measured the spot diameter at different positions, as shown in Fig. 4. According to the obtained beam diameters at different positions, the M^2 values were calculated to be ~1.5 in both horizontal and vertical directions.

We monitored the stability of the OPO output power for half an hour, shown in Fig. 5. Both the mode-locked $Nd:YVO_4$ laser and the OPO are exposed to the air. Compared with femtosecond pumping OPO, picosecond pumping OPO significantly reduced synchronization requirement between pump and signal and it was not sensitive to the environmental disturbance. The OPO output power was recorded every minute. In half an hour, the output power had a fluctuation of ±1.3%.

The wavelength tuning was performed by changing the MgO:PPLN crystal temperature at the fixed grating period of 31.5 μm. At the temperatures of 200 °C, 188° C, and 172°C, the signal and idler spectra were, respectively, presented in Fig. 6(a)–(c), and the corresponding average

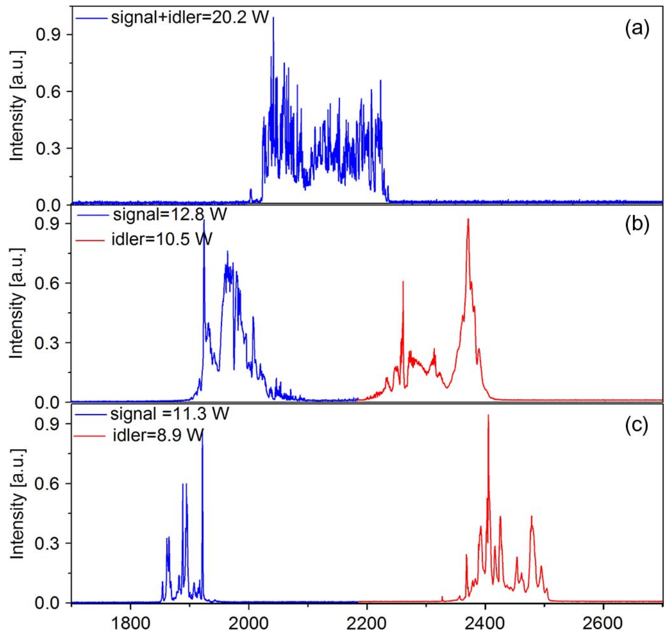

Fig. 6. Temperature–tuning spectra of the OPO.

output powers were also marked. The broad spectra in Fig. 6(a)–(c) could be attributed to the broad phase-matching bandwidth in degenerate or near-degenerate operation of the OPO. The total output power of signal and idler reached up to 23.3 W at 188 °C [see Fig. 6(b)], with a conversion efficiency of 76%. Compared with doubly resonant OPO in degeneracy, the singly resonant OPO was even more efficient because of the lower intra-cavity optical intensity. The slightly low output power at 172 °C [see Fig. 6(c)] was due to an increasing loss resulting from mirror coating which reflectivity decreased to 97% near 1860 nm. It was noticed that for different tuning wavelengths, the output powers of signal and idler were always stable.

It is noteworthy that due to phase conjugation of signal and idler in OPO, the high-power picosecond OPO system can be used for restoration of blurred images with high temporal resolution [17], [18]. In addition, it can also be used for generation of far infrared and THz waves by intracavity difference frequency generation of signal and idler pulses [19]–[21].

4. Conclusion

In conclusion, a high-average-power mid-infrared picosecond OPO was experimentally demonstrated. At the degenerate operation, the OPO delivered a maximum average output power of 20.2 W, with 29-ps pulse duration and 103-MHz repetition rate at the central wavelength of 2128 nm. To our best knowledge, this is the highest mid-infrared average output power from an ultrashort pulse OPO reported so far. In the non-degenerate operation, a signal power of 12.8 W (1966 nm) and an idler power of 10.5 W (2319 nm) were generated, with a conversion efficiency as high as 76%. This stable and high-power mid-infrared ultrafast OPO will be beneficial to the potential applications such as medical surgery, semiconductor material micro-processing, and so on.

References

[1] D. D. Arslanov *et al.*, “Continuous-wave optical parametric oscillator based infrared spectroscopy for sensitive molecular gas sensing,” *Laser Photon. Rev.*, vol. 7, no. 2, pp. 188–206, Mar. 2013.

[2] M. M. J. W. van Herpen, S. Li, S. E. Bisson, and F. J. M. Harren, “Photoacoustic trace gas detection of ethane using a continuously tunable, continuous-wave optical parametric oscillator based on periodically poled lithium niobate,” *Appl. Phys. Lett.*, vol. 81, no. 7, pp. 1157–1159, Aug. 2002.

[3] A. Berrou, M. Raybaut, A. Godard, and M. Lefebvre, “High-resolution photoacoustic and direct absorption spectroscopy of main greenhouse gases by use of a pulsed entangled cavity doubly resonant OPO,” *Appl. Phys. B*, vol. 98, no. 1, pp. 217–230, Jan. 2010.
[4] J. Hu, C. R. Menyuk, L. B. Shaw, J. S. Sanghera, and I. D. Aggarwal, “Computational study of 3–5 μm source created by using supercontinuum generation in As_2S_3 chalcogenide fibers with a pump at 2 μm,” *Opt. Lett.*, vol. 35, no. 17, pp. 2907–2909, Sep. 2010.
[5] K. L. Vodopyanov, I. Makasyuk, and P. G. Schunemann, “Grating tunable 4–14 μm GaAs optical parametric oscillator pumped at 3 μm,” *Opt. Exp.*, vol. 22, no. 4, pp. 4131–4136, Feb. 2014.
[6] K. Sugioka and Y. Cheng, “Ultrafast lasers—Reliable tools for advanced materials processing,” *Light Sci. Appl.*, vol. 3, pp. 30, Apr. 2014.
[7] Z. Qin *et al.*, “Diode-pumped passively mode-locked Tm:$CaGdAlO_4$ laser at 2-μm wavelength,” *IEEE Photon. J.*, vol. 7, no. 1, Feb. 2015, Art. ID. 1500205.
[8] V. Aleksandrov *et al.*, “Mode-locked Tm,Ho:$KLu(WO_4)_2$ laser at 2060 nm using InGaSb-based SESAMs,” *Opt. Exp.*, vol. 23, no. 4, pp. 4614–4619, Feb. 2015.
[9] J. Ma *et al.*, “Wavelength-versatile graphene–gold film saturable absorber mirror for ultra-broadband mode-locking of bulk lasers,” *Sci. Rep.*, vol. 4, p. 5016, May 2014.
[10] J. Li, D. D. Hudson, Y. Liu, and S. D. Jackson, “Efficient 2.87 μm fiber laser passively switched using a semiconductor saturable absorber mirror,” *Opt. Lett.*, vol. 37, no. 18, pp. 3747–3749, Sep. 2012.
[11] F. Ruebel, G. Anstett, and J. A. L'huillier “Synchronously pumped mid-infrared optical parametric oscillator with an output power exceeding 1 W at 4.5 μm,” *Appl. Phys. B*, vol. 102, no. 4, pp. 751–755, Mar. 2011.
[12] F. Kienle *et al.*, “High-power, variable repetition rate, picosecond optical parametric oscillator pumped by an amplified gain-switched diode,” *Opt. Exp.*, vol. 18, no. 8, pp. 7602–7610, Mar. 2010.
[13] O. Kokabee, A. Esteban-Martin, and M. Ebrahim-Zadeh, “Efficient, high-power, ytterbium-fiber-laser-pumped picosecond optical parametric oscillator,” *Opt. Lett.*, vol. 35, no. 19. pp. 3210–3212, Oct. 2010.
[14] K. Finsterbusch, R. Urschel, and H. Zacharias, “Fourier-transform-limited, high-power picosecond optical parametric oscillator based on periodically poled lithium niobate,” *Appl. Phys. B*, vol. 70, no. 6, pp. 741–746, Jun. 2000.
[15] C. W. Hoyt, M. Sheik-Bahae, and M. Ebrahimzadeh, “High-power picosecond optical parametric oscillator based on periodically poled lithium niobate,” *Opt. Lett.*, vol. 27, no. 17, pp. 1543–1545, Sep. 2002.
[16] B. Ruffing, A. Nebel, and R. Wallenstein, “All-solid-state cw mode-locked picosecond $KTiOAsO_4$(KTA) optical parametric oscillator,” *Appl. Phys. B*, vol. 67, no. 5, pp. 537–544, Nov. 1998.
[17] Y. J. Ding, “Phase conjugation based on single backward second-order nonlinear parametric process,” *Opt. Lett.*, vol. 37, no. 22, pp. 4792–4794, Nov. 2012.
[18] X. Zou *et al.*, “Restoration of blurred images due to phase distortion based on polarization-insensitive phase conjugation in second-order nonlinear medium,” *Opt. Lett.*, vol. 38, no. 16, pp. 3054–3056, Aug. 2013.
[19] P. Zhao, S. Ragam, Y. J. Ding, and L. B. Zotova, “Terahertz intracavity generation from output coupler consisting of stacked GaP plates,” *Appl. Phys. Lett.*, vol. 101, no. 2, Jul. 2012, Art. ID. 021107.
[20] R. Chen, G. Sun, G. Xu, Y. J. Ding, and L. B. Zotova, “Generation of high-frequency terahertz waves in periodically poled $LiNbO_3$ based on backward parametric interaction,” *Appl. Phys, Lett.*, vol. 101, no. 11, Sep. 2012, Art. ID. 111101.
[21] G. Xu, X. Mu, Y. J. Ding, and I. B. Zotova, “Efficient generation of backward terahertz pulses from multiperiod periodically poled lithium niobate,” *Opt. Lett.*, vol. 34, no. 7, pp. 995–997, Apr. 2009.